

[3+2] resonance enhanced multiphoton ionization of I and Br formed from the infrared multiphoton decomposition of CF₃I and CF₃Br

Robert M. Robertson, David M. Golden, and Michel J. Rossi

Citation: *The Journal of Chemical Physics* **89**, 2925 (1988); doi: 10.1063/1.454997

View online: <http://dx.doi.org/10.1063/1.454997>

View Table of Contents: <http://scitation.aip.org/content/aip/journal/jcp/89/5?ver=pdfcov>

Published by the [AIP Publishing](#)

Articles you may be interested in

Photodissociation dynamics of 3-bromo-1,1,1-trifluoro-2-propanol and 2-(bromomethyl) hexafluoro-2-propanol at 234 nm: Resonance-enhanced multiphoton ionization detection of Br (2 P j)

J. Chem. Phys. **134**, 194313 (2011); 10.1063/1.3591373

Infrared resonance enhanced multiphoton ionization of fullerenes

AIP Conf. Proc. **454**, 3 (1998); 10.1063/1.57178

A resonance enhanced multiphoton ionization study of the gerade excited states of Xe₂ with a Xe 1 S₀+Xe* 6s[3/2]₁ dissociation limit

J. Chem. Phys. **102**, 4020 (1995); 10.1063/1.468530

Polarizationresolved (2+1) resonanceenhanced multiphoton ionization spectroscopy of CF₃I (6s) Rydberg states

J. Chem. Phys. **98**, 4355 (1993); 10.1063/1.464997

Photofragmentation of CF₃I⁺ produced by resonant multiphoton ionization

J. Chem. Phys. **97**, 7263 (1992); 10.1063/1.463499



[3+ 2] resonance enhanced multiphoton ionization of I and Br formed from the infrared multiphoton decomposition of CF₃I and CF₃Br^{a)}

Robert M. Robertson,^{b)} David M. Golden, and Michel J. Rossi^{c)}

Department of Chemical Kinetics, Chemical Physics Laboratory, SRI International, Menlo Park, California 94025

(Received 29 March 1988; accepted 16 May 1988)

Resonance enhanced multiphoton ionization (REMPI) has been used to study the products of the infrared multiphoton decomposition (IRMPD) of CF₃I in a very low-pressure photolysis (VLPΦ) cell. The strongest REMPI signals are due to the ground state I(²P_{3/2}) and the spin-orbit excited state I*(²P_{1/2}). The origins of I and I* were determined from the time and IR laser fluence dependences of the REMPI signal. I* is formed by visible single photon dissociation of vibrationally excited CF₃I and by visible multiphoton dissociation of I₂ and thermal CF₃I. The ionization efficiency of I has been determined relative to NH₃ for our probe laser conditions, and the sticking coefficient of I with gold surfaces has been determined. The REMPI spectra of the products of the IRMPD of CF₃Br is also presented.

INTRODUCTION

Resonance enhanced multiphoton ionization (REMPI) has been used successfully in recent years as a diagnostic tool in kinetic systems, e.g., flames,¹ pyrolysis,² photodissociation,³ plasmas,⁴ surface scattering,⁵ and gas collisions.⁶ REMPI is advantageous in many instances because it provides high selectivity, sensitivity, and temporal resolution. Furthermore, the detection limits using REMPI are frequently lower than for luminescence measurements, and many nonfluorescing molecules can be detected with REMPI.

Recently we have begun to investigate the interaction of atoms and free radicals with surfaces in a very low-pressure photolysis (VLPΦ) cell. The transient species are created by infrared multiphoton decomposition (IRMPD) of an appropriate precursor in a collimated (unfocused) laser beam and are allowed to react with the cell walls or a temperature-controlled sample surface. Modulated molecular-beam mass spectrometry is used to monitor the effluents from the VLPΦ cell, and REMPI is used to monitor the transient species *in situ* and in real time. We are able to calibrate our REMPI signals in terms of absolute densities based on the mass spectrometer measurements of the precursor depletion. Knowledge of the absolute densities of transient species is necessary for the quantitative treatment of competitive first- and second-order kinetic processes inside the reactor.

In this paper the [3 + 2] REMPI spectra of I and I* atoms generated (directly or indirectly) by IRMPD of CF₃I are reported. The time and IR-fluence dependence of the REMPI signals is used to study the origin of the atoms. Due to the low-pressure conditions and the predominance of gas-wall collisions in the Knudsen cell, the I atoms are lost primarily to the vessel walls and the sticking coefficient for this reaction is determined. In the VLPΦ reactor, we are able to determine the absolute density of I formed by the IRMPD of

CF₃I. We use this to determine the ionization efficiency of I relative to a stable gas, NH₃, for our probe laser conditions. The REMPI spectra resulting from the IRMPD of CF₃Br is presented. The [3 + 1] REMPI⁷ of CF₃ was not observed from the IRMPD of either of these precursor gases, because of the background signal due to visible laser photodissociation/ionization of the precursors. We will discuss previous studies⁸⁻¹¹ of the REMPI of I and I* generated by the IRMPD of CF₃I. In another study¹² the REMPI spectra of CF₃ have been studied using hexafluoroacetone as the precursor. In these experiments, the gas-phase rate constant for CF₃ recombination was verified, the CF₃ REMPI signal was calibrated, and the etching of silicon by CF₃ radicals was quantitatively studied.

EXPERIMENTAL

The VLPΦ experiments were performed at low pressure ($< 2 \times 10^{-3}$ Torr) in a Knudsen reactor equipped with wire electrodes for the collection of ions and electrons. The cell, which has been described previously,¹² is an all stainless-steel six-way cross where four branches are fitted with windows for the crossed IR- and visible-laser beams. One branch is blanked off, and the other branch houses a butterfly valve with an interchangeable exit aperture mounted in the center. The cell walls have been coated with gold by vacuum evaporation in order to minimize CF₃ wall losses.

The ions and electrons created by REMPI were collected on two tantalum wire-loop electrodes that were placed above and below the intersection of the two lasers. The electrodes were biased at plus and minus 90 V for the collection of electrons and ions, respectively. The electrical currents were converted to voltages using a load resistor of $10^7 \Omega$, then the electron signal was inverted and added to the ion signal.¹³ The time dependence of the total REMPI signals following the dye laser pulse are shown in Fig. 1 for collection voltages of ± 9 and ± 90 V. The total charge was collected for high and low collection voltages. However, the signal amplitude was smaller at the lower collection voltage

^{a)} This work was supported by the Air Force Office of Scientific Research under Contract No. F49620-85-K-0001.

^{b)} Postdoctoral Research Associate.

^{c)} Corresponding author.

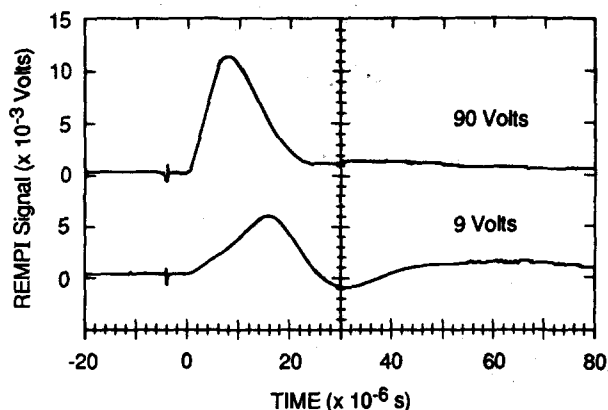


FIG. 1. I-atom REMPI signal at 474.5 nm (averaged over 128 shots) vs time after the probe laser is fired for collection voltages of ± 9 and ± 90 V. The conditions were: 4 mJ/pulse $F_{CF_3I} = 4 \times 10^{15} \text{ s}^{-1}$, $f = 12\%$, delay between IR and dye laser pulse was 3 μs .

due to the larger collection times. The signals obtained using the larger collection voltages were analyzed with a boxcar integrator (5 μs gate width and delay). The signal from the boxcar was calibrated in terms of the number of ion and electron pairs produced per dye laser pulse based on the amplifier gain and the relationship between the peak height and total area of the time-dependent signal. A boxcar signal of 1 mV represented 4300 ion/electron pairs. Shot-to-shot variations in the pulse energies of both lasers limited our sensitivity to 0.1 mV ($S/N = 1$).

The visible radiation for the multiphoton ionization process was generated by an excimer laser (Lumonics Hyperex 460 operated at 351 nm) pumped dye laser (Lambda Physik FL2002), generating up to 8 mJ per pulse. The IR radiation was generated by a Tachisto CO_2 -TEA laser (model 555) with pulse energies up to 1 J at the $R(12)$ or $R(16)$ line of the 9.6 μm band. Repetition rates were between 10 and 20 pps, and the delay time between the atom generating IR laser and the probe dye laser was varied using a digital delay generator. Scanning of the delay time with respect to the IR laser pulse resulted in the display of the temporal evolution of the REMPI signal. The visible laser focus (70 mm $f.l.$ lens) was positioned in the center of the IR-laser beam (cross sectional area of 1 cm^2).

RESULTS

CF_3I

The significant chemical reactions for the IRMPD of CF_3I are



I_w is an iodine atom adsorbed on a surface. The initial collisionless IRMPD occurs in the irradiated volume ($V_b = 20 \text{ cm}^3$) on the time scale of the pulse duration. In contrast to previous studies,^{9,11} we are able to monitor the I-atom gener-

ation during the IR-laser pulse, as well as after the pulse, because our irradiation conditions ($< 1 \text{ J/cm}^2$) do not lead to ac Stark shifting of the atom REMPI signals. The radical species and hot parent molecules, whose energy content is below the threshold for unimolecular decomposition, then mix throughout the cell volume ($V_c = 620 \text{ cm}^3$) on a time scale related to the molecular velocity and the dimensions of the cell (see below). Species with high sticking coefficients on the cold cell walls (> 0.1) are lost in this early period. Vibrationally excited species are thermalized after a small number of wall collisions. Thermal accommodation coefficients are typically greater than 0.1. The process of thermalization and mixing to form a uniform density in the cell is complete after several hundred μs . The species then undergo the reactions listed above until the next IR-laser shot occurs in 50 or 100 ms.

In previous¹⁴ modulated molecular-beam mass spectrometry studies of the type represented by Eqs. (1)–(5), only the stable products were monitored, and the key transient densities were inferred from the yields of the stable products. The application of REMPI to the study of these systems under the same reaction conditions is a major refinement of the experimental technique and allows for the direct observation of the reaction intermediates and the confirmation of the assumed reaction scheme.

CF_3I spectra and time dependence

The REMPI spectra of CF_3I has been studied under a variety of conditions in the wavelength range 460 to 490 nm (coumarin 480 dye). The spectra at 0.8×10^{-3} Torr of CF_3I are shown in Fig. 2 for the background (no IR laser) and two delay times. The IR laser was operated at 10 Hz and provided a CF_3I steady-state depletion (measured using the mass spectrometer) of 16%. The main difference between these two delay times is that at 0.3 μs the low-intensity tail of the IR pulse is still present and decomposition is still occurring. The species that are present in the probe volume at both of these early times are precursor gas molecules (thermal or vibrationally excited), stable product molecules from previous IR laser shots, and the nascent products of the decomposed CF_3I . Also shown in Fig. 2 are the expected wavelengths^{7,15} for the multiphoton ionization of CF_3 , ground-state iodine [$\text{I } 5p^5(^2P_{3/2})$], and the spin-orbit excited state [$\text{I}^* 5p^5(^2P_{1/2})$].

In the following sections, the five major peaks in the REMPI spectra are identified by wavelength and temporal behavior. Two of the peaks are identified as resulting from the ionization of I through three-photon resonant states $6s(^2P_{1/2})$ at 474.8 nm and $6s(^4P_{3/2})$ at 485.3 nm. These features were also seen by Hackett *et al.*,⁸ in a focused CO_2 -laser IRMPD experiment. Both lines are asymmetric and blue degraded, which is an indication of ac Stark broadening.¹⁶ Also, the 485.3 nm peak shows a spike on the red edge, reminiscent of the sharp features in the REMPI spectra of Ba that have been analyzed in terms of channel interference effects by Kelly, Hessler, and Alber.¹⁷ The narrow width of this peak suggests that it may not simply be the [4 + 1] REMPI feature expected at this wavelength.¹¹ Both of these features are present in the background spectrum to a lesser

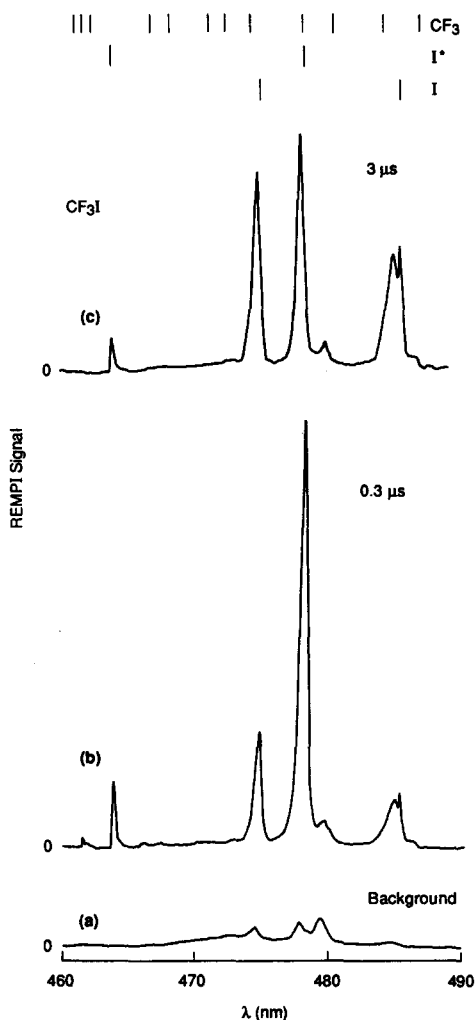


FIG. 2. REMPI spectra of CF_3I : (a) background (IR laser off); (b) IR laser on, probe laser delayed by $0.3 \mu\text{s}$; (c) IR laser on, probe laser delayed by $3 \mu\text{s}$. $P = 0.8 \times 10^{-3}$ Torr, $f = 16\%$, dye laser energy of 5.5 mJ/pulse .

extent, where they are thought to result from I produced by the visible two-photon excitation of CF_3I into the predissociative molecular state with ensuing rapid decomposition into CF_3 and iodine atoms (I and I^*).¹⁸ Single-photon dissociation is unlikely for ground-state CF_3I because of the low absorption of CF_3I in this wavelength range.^{19,20} The width of the REMPI lines are broader than the probe laser bandwidth (0.2 cm^{-1}) and are apparently due to ac Stark broadening by the focused dye laser and not by the (unfocused) IR irradiation. This conclusion also follows from a comparison of the peak widths of the REMPI spectrum of CF_3I with and without ("background" spectrum in Fig. 2) IR-laser irradiation.

The difference signal (IR laser on minus IR-laser off) of the I feature at 474.5 nm versus the delay time of the probe laser pulse is shown in Fig. 3 for the three IR laser fluences of 1.34 , 0.67 , and 0.22 J cm^{-2} , with parent gas depletions of 16% , 4% , and $<1\%$, respectively. The REMPI signal was taken at the peak of the line with a wavelength of 474.5 nm , 0.3 nm to the blue of the expected wavelength. At the highest fluence, the signal rises during the first few μs , decreases gradually during the next few hundred μs , and then remains

constant within experimental uncertainty until the next laser pulse. For the two lower fluence cases, the difference signal rises during the first few microseconds and then gradually falls to zero. The constant portion of the signal at late time for the high fluence case is due to a stable product of the IRMPD induced chemistry I_2 , whose presence we detect by mass spectrometry. We do not expect REMPI signals due to the molecular ion I_2^+ in this wavelength range because all accessible electronic states²¹ of I_2 at the two-photon level are predissociative leading to I and I^* . At late times, i.e., at several ms, essentially no difference signal is observed for the two lower fluence cases because there is no significant build up of I_2 . The REMPI signals at early time, late time, and without the IR laser all show a third-order formal intensity dependence on dye laser pulse energy with a slight turnover toward saturation at 5 to 6 mJ/pulse .

There are two sources of the difference signal at early times before any collisions occur: I generated from IRMPD of CF_3I and I generated by visible single-photon excitation and predissociation of the "hot" CF_3I prepared by IR excitation. The existence of the second mechanism is shown by previous experiments^{19,20} that showed a dramatic long wavelength shift in the UV absorption spectra with internal energy. Also, it will be shown below that this second mechanism must be occurring to explain our REMPI observations of I^* .

Two peaks in the REMPI spectrum of Fig. 2 arise from the ionization of I^* through three-photon resonant states $7s(^2P_{3/2})$ at 463.7 nm and $6s(^2S_{1/2})$ at 478.1 nm . The more intense peak has the characteristic line shape due to ac Stark broadening. The peak at 463.7 nm is weaker because of probe laser energy limitations in this wavelength range but nevertheless shows the same broadening and temporal dependence as the strong peak at 478.1 nm . In analogy with the ground-state I-atom REMPI signal discussed above, the origin of the REMPI signal corresponding to I^* in the CF_3I background spectrum [Fig. 2(a)] is due to two-photon dissociation and subsequent ionization by the probe laser pulse.

In Fig. 3 the time dependence of the REMPI difference signal for I^* is shown for three values of the IR-laser fluence. This signal was monitored at 477.8 nm , shifted 0.3 nm due to the Stark effect. At the two low fluences, the REMPI difference signal rises in the first few μs and then gradually decreases to zero in analogy to I atom REMPI discussed above. At the highest laser fluence the signal rises to a maximum at about $0.5 \mu\text{s}$ then sharply decreases over the next $1 \mu\text{s}$. After this early period the signal behaves similarly to the 474.5 nm REMPI signal due to ground state I, decreasing gradually to 1 ms and then remaining constant until the next laser shot. The late time constant signal is due to I_2 , as discussed above for I. The origin of the large REMPI difference signal in the collisionless regime (a few μs after IR excitation) is due to I^* generated by visible single-photon decomposition of IR-laser excited CF_3I . At the highest IR fluence the 477.8 nm REMPI signal increases during the first $0.5 \mu\text{s}$ as the average internal energy of CF_3I increases due to IR pumping. The signal then decreases over the next $2 \mu\text{s}$ as excited CF_3I continues to decompose during the duration of the IR laser pulse. For the lower IR-fluence conditions we only observe an increase in REMPI signal as the CF_3I heats up with very

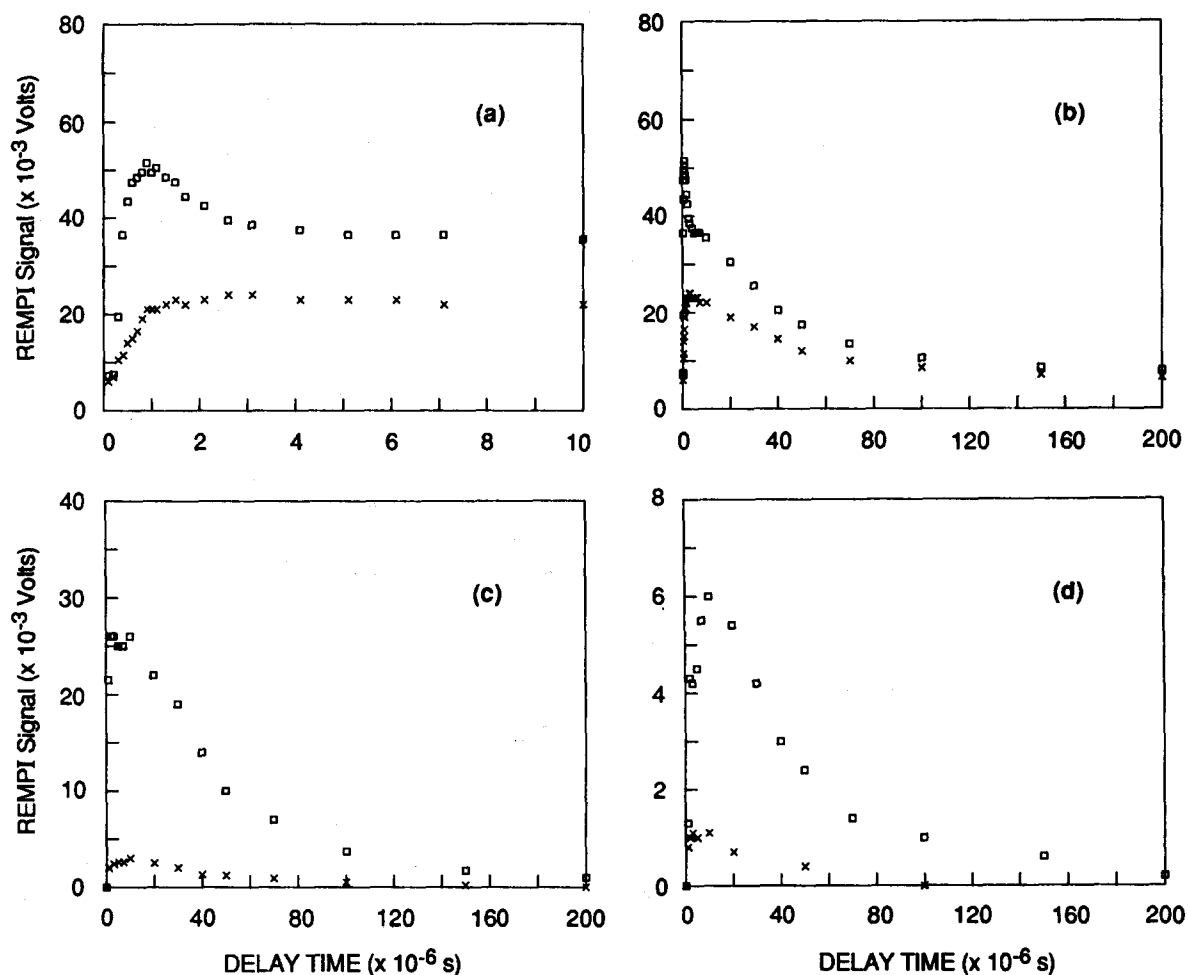


FIG. 3. REMPI difference signals (IR laser on minus IR laser off) for I (474.5 nm, \times) and I* (477.8 nm, boxes) vs probe laser delay. (a) and (b) IR laser fluence Φ_0 of 1.34 J cm^{-2} , $f = 16\%$; (c) Φ_0 of 0.67 J cm^{-2} , $f = 4\%$; (d) Φ_0 of 0.22 J cm^{-2} , $f < 1\%$. $F_{CF,I} = 4 \times 10^{15} \text{ s}^{-1}$, 6 mJ/pulse dye laser energy, 11 pps.

little IRMPD occurring. Contrary to the report by Boriev *et al.*,²² we do not believe that I* can be generated from the IRMPD of CF_3I because the threshold energy for this process is significantly higher (by 7600 cm^{-1}) than for I. In agreement with REMPI signals for I, the I* REMPI signal followed a third-order formal intensity law as a function of dye-laser pulse energy under all experimental conditions.

The REMPI signal at 479.6 nm in Fig. 2 is assigned to an unspecified resonance of the CF_3I molecule. Its wavelength position does not correspond to either an I or I* resonance. Furthermore, the signal decreases when the IR laser is turned on, and the short time delay signal is smaller than at long delay times. Thus, this signal cannot be due to CF_3 or any other product formed by IRMPD of CF_3I . We also note that the peak shape is symmetric in contrast to the Stark shifted lines discussed above.

CF_3Br spectra

The REMPI spectrum of CF_3Br has been studied using focused and unfocused CO_2 laser radiation. Focused IR radiation was used to achieve higher degrees of decomposition of the parent gas in the focal volume. Under these circumstances, it was necessary that the focus of the dye laser be

located in the focal volume of the CO_2 laser. The spectra for both conditions are shown in Fig. 4 along with a background spectrum. Also shown in Fig. 4 are the wavelengths^{7,15} where REMPI signals are expected for CF_3 , ground-state Br ($^2P_{3/2}$) and excited-state Br, Br* ($^2P_{1/2}$).

The only strong REMPI signal seen under focused CO_2 laser conditions is identified as the [3 + 2] REMPI of the ground-state Br through the $5s(^4P_{3/2})$ state at 462.3 nm. As for I atom REMPI, the atomic resonance is considerably broadened and Stark shifted.¹⁶ The absence of a peak at 473 nm corresponding to the [3 + 2] REMPI via the resonant $^4P_{5/2}$ state in Br is due to the low probe laser power for the experimental conditions of Fig. 4. In a scan with a different dye (coumarin 480), a weak signal was observed at 473 nm but was not studied in detail. The absence of the REMPI signal at 459.6 nm corresponding to [3 + 2] REMPI of Br in the upper spin state via the resonant $5s^2P_{1/2}$ state can be explained by the fact that the focused IR radiation bleaches the probed volume thus photolyzing all irradiated CF_3Br molecules. In this case, no vibrationally excited CF_3Br molecules remain that could undergo single-photon dissociation with subsequent [3 + 2] REMPI of Br*, in complete analogy to the experimental situation of Hackett and co-workers⁹

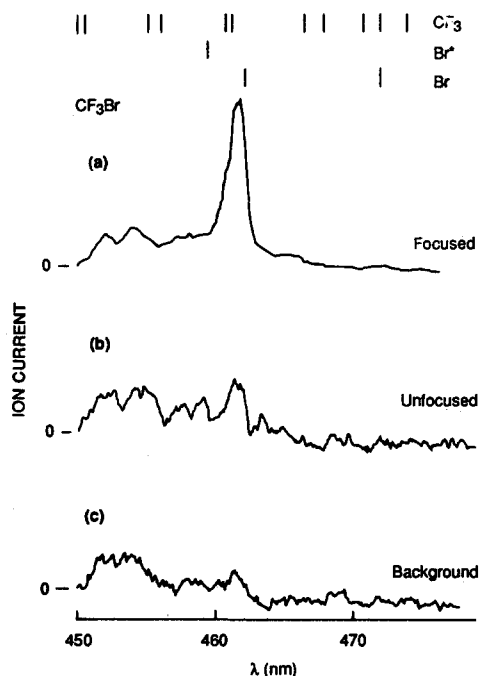


FIG. 4. REMPI spectra of CF_3Br ; IR laser off, collimated, and focused. The delay time for the probe laser was $3 \mu\text{s}$. The expected line positions for CF_3 , Br, and Br^* are shown at the top of the figure.

for the case of CF_3I . The absence of strong REMPI signals due to CF_3 free radicals is apparently due to the large background signal from CF_3Br REMPI.

In the spectrum obtained with the collimated IR-laser beam the line at 462.3 nm for Br is weaker because the extent of CF_3Br depletion is smaller. We find a small signal at the wavelength expected for REMPI of Br^* under collimated IR-laser conditions. In the background spectrum for CF_3Br , we observe the signal for the ionization of Br and Br^* albeit at reduced signal to noise. As in CF_3I , the halogen atoms can also be generated by visible two-photon dissociation of CF_3Br as observed in the background spectrum of Fig. 4.

DISCUSSION

Since we use the REMPI signal at 474.5 nm as a measure of the density of the ground-state I atom, and since we use the time history of this signal to extract both sticking coefficient and ionization efficiency, we begin with the justification of the assignment of the REMPI signals. From the discussion of the IR fluence and time dependence in the previous section, it is apparent that the difference REMPI signal at 474.5 nm monitors the density of I atoms formed by IRMPD; whereas the corresponding signal at 477.8 nm monitors the vibrationally excited parent molecule CF_3I . From the literature, two facts are known with certainty: First, the absorption spectrum of CF_3I strongly shifts towards the red upon internal excitation^{19,20} such that IR-multiphoton excited CF_3I decomposes upon single-photon absorption around 475 nm. Second, the quantum yields for I^* generation following predissociation via the *A* state has been measured for a great number of generic alkyl iodides with increasing accuracy^{23,24} and is 0.92 for CF_3I .¹⁸

The quantum yield changes with excitation wavelength, e.g., it drops from 1.0 to 0.6 from 300 to 336 nm for $\text{C}_3\text{F}_7\text{I}$. Although this behavior has not been established for CF_3I , it is very likely that it is similar in light of a recent investigation of the composite nature of the *A* state in CF_3I by Van Veen.¹⁸ Because the quantum yield of I is small and does not change significantly with excitation wavelength, we interpret the time dependence of the REMPI signal at 474.5 nm during the IR-laser pulse as reflecting the kinetics of formation of I atom from IRMPD of CF_3I with essentially no interference from the complicating contribution of hot CF_3I under high IR-laser fluence conditions. We further justify this conclusion by the fact that the REMPI signal at 474.5 nm and under conditions of high IR-laser fluence, does not show the characteristic rise and fall during the IR-laser pulse exhibited by the REMPI signal at 477.8 nm. This latter originates from a single process, which is photodissociation of vibrationally highly excited CF_3I . On the other hand, the signal at 474.5 nm is a superposition of REMPI signals of ground-state I atoms from both IRMPD of CF_3I and single-photon dissociation¹⁸ of CF_3I^+ ($\sim 8\%$). The small contribution from the latter can also be seen when one considers the small REMPI signal amplitude at 474.8 nm when the IR fluence is low and the IRMPD yield is vanishingly small. The ratio of REMPI signals at 477.8 and 474.5 nm further demonstrates the small I atom yield from the single-photon dissociation of CF_3I^+ [Figs. 3(c) and 3(d)].

The rise and fall of the REMPI signal at 477.8 nm within the IR-laser pulse is due to the fact that the IR-pumping process generates hot CF_3I and also causes its loss upon further pumping by IRMPD. The temporal behavior of this REMPI signal is thus dependent upon IR-laser fluence. At low fluence, where no decomposition takes place, the signal reaches a constant level, whereas under conditions of significant IRMPD [16%, Fig. 3(a)] the REMPI signal decreases substantially due to depletion of the pool of reacting molecules. It is not straightforward to model the time dependence of this REMPI signal, because it depends not only on the resonant ionization of I, but also on the single-photon dissociation of hot CF_3I that has not been studied in detail. Moreover, there exists the distinct possibility that the branching ratio is dependent on the internal energy of CF_3I which by itself could lead to a time dependence such as presented in Fig. 3 for the 477.8 nm REMPI signal. The reason we give only a qualitative explanation at this point is the fact that REMPI of CF_3I^+ (hot) is a complex process which depends on the properties of the hot precursor and its photodissociation product.

Thus far only the short time dependence of the REMPI signal within the IR-laser pulse has been discussed. Both the irradiated (hot) molecules, as well as the photoproducts formed within the irradiated volume up to the end of the collisionless IRMPD expand into the rest of the Knudsen cell, which has a ratio of 31:1 in terms of total volume to irradiated volume. This decrease of the original density of transient species is described by the temporal dependence of the REMPI signal on the time scale of several hundred μs . The decay constant k_d is given by Eq. (6) assuming Maxwellian flow at ambient temperature, which is expected to

hold for the present case of a simple bond fission reaction, under conditions of negligible translational energy release:

$$k_d = (3\langle v \rangle) / 4R. \quad (6)$$

$\langle v \rangle$ is the molecular velocity and R is the radius of a sphere of irradiated molecules. This equation also holds²⁵ for cylindrical geometry of a cylinder of radius R and length $2R$. It is important to describe this relaxation to homogeneous density throughout the reactor in analytical terms in order to separate the heterogeneous interaction from homogeneous mixing. If this separation of kinetic processes cannot be achieved, we would be unable to obtain quantitative results for the heterogeneous interaction of the transients with the cell walls. One of the conditions where this separation would not be possible corresponds to the situation where the sticking coefficient γ is on the order of 0.3, in which case the rate of the heterogeneous reaction is faster or of the same magnitude as the rate of homogeneous mixing. Experimentally, this separation of kinetic processes into two distinctly different time domains manifests itself in a break of a logarithmic plot of the transient density vs time. The faster decay process pertains to k_d , whereas the slower process obtains the rate constant for the heterogeneous interaction, which is the quantity of interest.

Table I presents our data in terms of observed and calculated k_d values with the above justified assumption that the REMPI signal at 474.5 nm and high IR-laser fluence is due to the I atom, whereas all other experimental situations at both 474.5 and 477.8 nm correspond to $\text{CF}_3\text{I}^\ddagger$ (i.e., $\langle v \rangle$ is calculated using the mass of I or CF_3I). Row (a) in Table I corresponds to high IR-laser fluence with concomitant 16% IRMPD, whereas row (b) corresponds to low IR-laser fluence with essentially no IRMPD, hence no I-atom formation. We note the close agreement between observed and calculated decay rate constants which also supports our contention that the I-atom contribution probed at 474.5 nm in the single-photon dissociation of $\text{CF}_3\text{I}^\ddagger$ is small. This supports our suggestion regarding the REMPI signal intensity at 474.5 nm at high IR fluence as representative of the I-atom density.

Sticking coefficient

Since Eq. (6) describes the homogeneous mixing process adequately, we will now discuss the I-atom density as a function of time after homogeneous mixing has been achieved. Various chemical and physical processes can take place after this mixing process is completed, and when one compares the REMPI signal at 474.5 vs 477.8 nm, we obtain a first-order loss rate constant k_w for I-atom loss of 77 and 407 s^{-1} , respectively, under two sets of conditions from two separate experiments. These values are approximate because

TABLE I. Decay constant (units of 10^{-4}s^{-1}).

	k_d^{474}	k_d^{474} (calc)	k_d^{478}	k_d^{478} (calc)
(a)	2.7 ± 0.5	3.0	2.3 ± 0.2	2.4
(b)	2.3 ± 0.3	2.4	2.3 ± 0.3	2.4

the present cell does not have the required sensitivity to measure this quantity with high accuracy due to the small irradiated volume with respect to the total cell volume. The REMPI signal at 477.8 nm representing $\text{CF}_3\text{I}^\ddagger$ vanishes after several hundred μs indicating that the sticking coefficient for hot CF_3I is >0.3 . We relate our measured quantity k_w to γ by dividing it by the gas-wall collision frequency $\omega = 4240 \times (T/M)^{1/2}$ resulting in values of 1.2×10^{-2} and 6.2×10^{-2} , respectively.

Houston and co-workers have studied the vibrational relaxation of vibrationally excited CO_2 on Ag and other surfaces²⁶ and have related k_w to the surface deactivation probability γ using Eq. (7):

$$\gamma = 1 - \exp(-k_w d / \langle v \rangle), \quad (7)$$

where $\langle v \rangle$ is the two-dimensional molecular velocity and d is the cell diameter (6.3 cm). Using Eq. (7), we obtain essentially the same values for γ of I as above.

There is no doubt that k_w corresponds to adsorption of atomic I on the walls of the reaction vessel of which 90% are gold, along with some quartz and KCl windows for laser beam throughput. Even though our surfaces are not well characterized at this point our γ values give a useful range for this important parameter. The reason for attributing k_w to a heterogeneous process is the fact that homogeneous recombination of I at those pressures is very slow. With a third-order (homogeneous) rate constant for I recombination²⁷ (I_2 as third body) of $8.3 \times 10^{-32} \text{cm}^6 \text{s}^{-1}$, we calculate an effective first-order recombination rate constant of $1.5 \times 10^{-4} \text{s}^{-1}$, which is five to six orders of magnitude slower than the measured decay rate constant for I disappearance in our cell. It therefore appears reasonable to identify this loss process as a heterogeneous process.

We also observe I_2 in the cell some time after the onset of IRMPD, but we cannot determine the branching ratio for I_2 formation. A hint that not all I atoms adsorbed on the gold surface recombine to I_2 is the fact that we observe CF_3I by mass spectrometry upon IRMPD of hexafluoroacetone in the cell that had been exposed previously to IRMPD of CF_3I , hence to a healthy I-atom flux. This also means that the present surface has the ability to "store" I atoms that recombined with CF_3 radicals in a heterogeneous manner after the cell had been pumped out overnight between the CF_3I and the hexafluoroacetone IRMPD experiment.

Relative ionization efficiency

Relative or absolute ionization efficiencies of I atoms can be determined if the density of I and the REMPI signal intensity are known. The density of I generated in the IR beam volume is given by Eq. (8):

$$[\text{I}] = fF_{\text{CF}_3\text{I}} t_p / V_b, \quad (8)$$

where t_p is the period of the laser, f the fractional decomposition, $F_{\text{CF}_3\text{I}}$ the flow rate of CF_3I , and V_b the originally irradiated beam volume. For the highest fluence data in Fig. 3(a), we calculate a density of I in the IR beam of $2.9 \times 10^{12} \text{cm}^{-3}$.

At high IR fluence, the early time increase in the REMPI signal at 474 nm is primarily due to IRMPD. There-

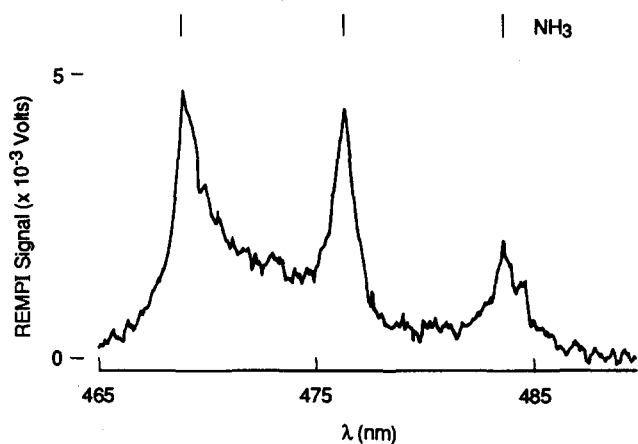


FIG. 5. REMPI spectrum of NH_3 at 0.5×10^{-3} Torr, 8 mJ/pulse, and 11 pps.

fore, we can assess the amount of signal that is due to I atoms from IRMPD (23–7 mV). We determine the relative ionization probability using NH_3 as a standard that also has [3 + 2] REMPI signals with the same formal intensity law as I, I^* in this wavelength region.²⁸ A REMPI spectrum of NH_3 is shown in Fig. 5. Using the REMPI signal at 476 nm (4.5 mV), the ratio of ionization probabilities is given by Eq. (9):

$$\frac{\text{Prob}(\text{I})^{474.5}}{\text{Prob}(\text{NH}_3)^{476}} = \frac{\text{Sig}_{\text{ion}}/[\text{I}]E_{\text{pulse}}^3}{\text{Sig}_{\text{ion}}/[\text{NH}_3]E_{\text{pulse}}^3} \quad (9)$$

The quantities in this expression are easily determined for our conditions resulting in an I atom ionization probability of 48 at 474.8 nm relative to NH_3 ionization at 476 nm in a [3 + 2] fashion.

¹K. C. Smyth and P. H. Taylor, *Chem. Phys. Lett.* **122**, 518 (1985).

²M.-S. Chou, *Chem. Phys. Lett.* **114**, 279 (1985).

- ³T. A. Spiglanin, R. A. Perry, and D. W. Chandler, *J. Chem. Phys.* **87**, 1568 (1987).
- ⁴J. H. M. Bonnie, E. H. A. Granneman, and H. J. Hopman, *Rev. Sci. Instrum.* **58**, 1353 (1987).
- ⁵J. S. Hayden and G. J. Diebold, *J. Chem. Phys.* **77**, 4767 (1982).
- ⁶E. E. Marinero, C. T. Rettner, and R. N. Zare, *J. Chem. Phys.* **80**, 4142 (1984).
- ⁷M. T. Duignan, J. W. Hudgens, and J. R. Wyatt, *J. Phys. Chem.* **86**, 4156 (1982).
- ⁸P. A. Hackett, P. John, M. Mayhew, and D. M. Rayner, *Chem. Phys. Lett.* **96**, 139 (1983).
- ⁹D. M. Rayner and P. A. Hackett, *Chem. Phys. Lett.* **110**, 482 (1984).
- ¹⁰M. Quack, E. Sutcliffe, P. A. Hackett, and D. M. Rayner, *Faraday Discuss. Chem. Soc.* **82**, 229 (1986).
- ¹¹D. M. Rayner and P. A. Hackett, *Isr. J. Chem.* **24**, 232 (1984).
- ¹²R. M. Robertson, D. M. Golden, and M. J. Rossi, *J. Vac. Sci. Technol. A* (accepted); *J. Phys. Chem.* (submitted).
- ¹³T. E. Adams, R. J. S. Morrison, and E. R. Grant, *Rev. Sci. Instrum.* **51**, 141 (1980).
- ¹⁴N. Selamoglu, M. J. Rossi, and D. M. Golden, *Chem. Phys. Lett.* **124**, 68 (1986).
- ¹⁵C. E. Moore, *Atomic Energy Levels*, Natl. Stand. Ref. Data Ser., Natl. Bur. Stand. No. 35 (U.S. GPO, Washington, D.C., 1971), Vols. 2 and 3.
- ¹⁶V. N. Bagratashvili, S. I. Ionov, G. V. Mishakov, and V. A. Semchin, *J. Opt. Soc. Am.* **4**, 129 (1987).
- ¹⁷J. F. Kelly, J. P. Hessler, and G. Alber, *Phys. Rev. A* **33**, 3913 (1986).
- ¹⁸G. N. A. Van Veen, T. Baller, A. E. DeVries, and M. Shapiro, *Chem. Phys.* **93**, 277 (1985).
- ¹⁹H. Pummer, J. Eggleston, W. K. Bischel, and C. K. Rhodes, *Appl. Phys. Lett.* **32**, 427 (1978).
- ²⁰I. N. Knyazev, Yu. A. Kudryavtsev, N. P. Kuzmina, and V. S. Letokhov, *Sov. Phys. JETP* **49**, 650 (1979).
- ²¹R. S. Mulliken, *J. Chem. Phys.* **55**, 288 (1971).
- ²²I. A. Boriev, A. M. Velichko, E. B. Gordon, A. A. Nadeikin, A. I. Nikitin, and V. L. Talroze, *JETP Lett.* **37**, 259 (1983).
- ²³J. E. Smedley and S. R. Leone, *J. Chem. Phys.* **79**, 2687 (1983).
- ²⁴W. P. Hess, S. J. Kohler, H. K. Haugen, and S. R. Leone, *J. Chem. Phys.* **84**, 2143 (1986); W. P. Hess and S. R. Leone, *ibid.* **86**, 3773 (1987).
- ²⁵H. Loehmannsroeben, K. Luther, and M. Stuke, *J. Phys. Chem.* **91**, 3499 (1987).
- ²⁶J. Misewich, C. N. Plum, G. Blyholder, P. L. Houston, and R. P. Merrill, *J. Chem. Phys.* **78**, 4245 (1983); J. Misewich, P. L. Houston, and R. P. Merrill, *ibid.* **82**, 1577 (1985).
- ²⁷J. Troe, *Annu. Rev. Phys. Chem.* **29**, 223 (1978).
- ²⁸J. H. Glowina, S. J. Riley, S. D. Colson, and G. C. Nieman, *J. Chem. Phys.* **73**, 4296 (1980).